SAKARYA ÜNİVERSİTESİ FEN BİLİMLERİ ENSTİTÜSÜ DERGİSİ
SAKARYA UNIVERSITY JOURNAL OF SCIENCE

e-ISSN: 2147-835X
Dergi sayfası: http://dergipark.gov.tr/saufenbilder

Geliş/Received
28.02.2017
Kabul/Accepted
25.04.2017

Doi
10.16984/saufenbilder.295487

Seebeck coefficient of $Ca_{2.8}Pr_{0.2}Co_4O_9$ synthesized by sol-gel method with thermal and structural characterization*

Enes Kilinc**[1] , M. Abdullah Sari[2], Fatih Uysal[1], Erdal Celik[3,4,5], Huseyin Kurt[1]

ABSTRACT

In this paper, $Ca_{2.8}Pr_{0.2}Co_4O_9$ powders were synthesized by sol-gel method and thermal and structural characterization of the powders were systematically examined for high temperature thermoelectric generator applications. Differential Thermal Analysis-Thermogravimetry (DTA-TG) was used to specify appropriate thermal regime of the powders for calcination process. Chemical structure and reaction type of intermediate temperature products were defined by Fourier Transform Infrared (FTIR) Spectroscopy. Structural properties of the powders were implemented by X-ray Diffraction (XRD) and X-ray Photoelectron Spectroscopy (XPS) was used to specify chemical composition and empirical formula of the elements existed within the powders. It can be seen from the phase spectrum that 2θ peaks of $Ca_{2.8}Pr_{0.2}Co_4O_9$ correspond to the literature and coincide with typical $Ca_3Co_4O_9$ peaks. Seebeck coefficients of the samples are much higher than $Ca_3Co_4O_9$ while they are closer to literature value of $Ca_{2.8}Pr_{0.2}Co_4O_9$. The highest Seebeck coefficient of $Ca_{2.8}Pr_{0.2}Co_4O_9$ is found to be 179 µV/K at 400 °C which is a little higher than the literature value. These results show that Pr is an effective dopant to increase the Seebeck coefficient values.

Keywords: Seebeck coefficient, sol-gel process, oxide thermoelectrics, thermal analysis.

---

* This study has been derived from the proceeding of “Sol-Gel Synthesis of $Ca_{2.8}Pr_{0.2}Co_4O_9$ Powders with Thermal and Structural Characterization” presented in the 4th International Symposium on Innovative Technologies in Engineering and Science (ISITES 2016).

** Corresponding Author: Address: Karabuk Universitesi, Muhendislik Fakultesi, Makina Muhendisligi Bolumu, Oda No: 348, 78050, Karabuk, Turkey. E-mail address: eneskilinc@karabuk.edu.tr.

[1] Faculty of Engineering, Department of Mechanical Engineering, Karabuk University, Karabuk, Turkey.

[2] The Graduate School of Natural and Applied Sciences, Department of Metallurgical and Materials Engineering, Dokuz Eylul University, Izmir, Turkey.

[3] Center for Production and Application of Electronic Materials (EMUM), Dokuz Eylul University, Izmir, Turkey.

[4] Faculty of Engineering, Department of Metallurgical and Materials Engineering, Dokuz Eylul University, Izmir, Turkey.

[5] The Graduate School of Natural and Applied Sciences, Department of Nanoscience & Nanoengineering, Dokuz Eylul University, Izmir, Turkey.

1. INTRODUCTION

Thermoelectric (TE) materials have attracted a great deal of attention by converting heat energy into electrical energy directly for TE power generation applications [1]. If p- and n-type materials are connected electrically in series and thermally in parallel coupled with a temperature difference applied between two sides of a thermoelectric generator (TEG), an output voltage is produced. This impact is called the Seebeck effect [2]. Efficiency of a TE material is evaluated by dimensionless figure of merit (zT) defined as

$$zT = \frac{S^2T}{\rho\kappa} \tag{1}$$

where S is the Seebeck coefficient, ρ is the electrical resistivity, κ is the thermal conductivity, and T is the temperature. A TE material should have high Seebeck coefficient and low electrical resistivity associated with low thermal conductivity [3].

Recently, TE oxides became advantageous over alloy based intermetallic compounds in terms of high temperature stability, cost of starting materials, easy manufacturing and high temperature application areas [4]. Having looked at oxide TE materials, $Ca_3Co_4O_9$ [5] and ZnO [6] have become important candidates for p- and n-type oxide TE materials with high zT values at high temperatures. In the past decade, many methods including doping have been used to improve their TE properties. Doping methods are the major approach to improve zT of bulk materials [7]. Through these studies, zT values of bulk oxide TE materials have reached to 0.5 at 1000 K and 0.65 at 1247 K for p-type $Ca_{2.7}Ag_{0.3}Co_4O_9$/Ag-10 wt.% composite [8] and n-type $Zn_{0.96}Al_{0.02}Ga_{0.02}O$ [9], respectively.

Over the past decades, many synthesis methods have been used to synthesize $Ca_3Co_4O_9$ and ZnO powders such as solid state reaction method [10], self-ignition method [11], combustion synthesis method [12], and sol-gel method [13]. Between these methods, sol-gel synthesis has some advantages among them as better stoichiometry control and homogeneity, lower reaction temperatures, easy fabrication and opportunity of using high-purity precursors [14]. High gas pressure can be applied isostatically along with high temperatures to all surfaces of a sample by hot isostatic pressing (HIP) to obtain bulk samples [15].

In this study, p-type $Ca_{2.8}Pr_{0.2}Co_4O_9$ was manufactured using sol-gel synthesis and HIP in order to investigate TE property of Seebeck coefficient for TEG applications. Synthesis and characterization of $Ca_{2.8}Pr_{0.2}Co_4O_9$ were performed systematically using Ca, Pr and Co based precursors to identify solution characteristics, process regime, structural properties and elemental composition of the powders. Within this scope, solution characteristics of the precursors were determined by pH and turbidity measurements. Thermal properties of the powders were characterized by Differential Thermal Analysis-Thermogravimetry (DTA-TG) in order to obtain appropriate calcination regime and Fourier Transform Infrared (FTIR) Spectroscopy was used to define chemical structure and reaction type of intermediate temperature products. Structural analysis of the $Ca_{2.8}Pr_{0.2}Co_4O_9$ powders was carried out using X-ray Diffraction (XRD) and results were compared with literature. X-ray Photoelectron Spectroscopy (XPS) was used to specify elemental composition and empirical formula of the elements within the powders. HIP was used to consolidate the powders. In addition to chemical characterizations, Seebeck coefficient values of the bulk samples were observed from 373 K to 673 K to investigate the effects of the fabrication methods and doping of $Ca_{2.8}Pr_{0.2}Co_4O_9$ samples.

2. MATERIALS AND METHOD

In this study, $Ca_{2.8}Pr_{0.2}Co_4O_9$ powders were synthesized using sol-gel method. Calcium nitrate tetra hydrate (99%, Alfa Aesar), praseodymium (III) nitrate hydrate (99.9%, Alfa Aesar) and cobalt (II) nitrate hexahydrate (ACS, Alfa Aesar) were used in stoichiometric ratios as starting materials to obtain 0.02 mole $Ca_{2.8}Pr_{0.2}Co_4O_9$. Distilled water was used as the solvent to dissolve each precursor having fully dispersed and homogenous solutions. After obtaining separate solutions of the precursors, the solutions were mixed and magnetically stirred at 100 °C to obtain final homogeneous solution and citric acid monohydrate was added as chelating agent to accelerate xerogel formation. After gelation process, obtained xerogel was dried at 200

°C for 2 h to remove moisture and undesired gases and $Ca_{2.8}Pr_{0.2}Co_4O_9$ powders were obtained. Amounts of the precursors, solvent and chelating agent were given in **Table 1**.

Table 1. Stoichiometric ratios used for 0.02 mole of $Ca_{2.8}Pr_{0.2}Co_4O_9$ powders.

Precursors	**Molecular Weight (g/mole)**	**Amount**
Calcium nitrate tetra hydrate	236.15	13.2244 g
Praseodymium (III) nitrate hydrate	291.04	23.2832 g
Cobalt (II) nitrate hexahydrate	326.92	1.3077 g
Distilled water	18	200 ml
Citric acid monohydrate	210.14	4.2028 g

Solution characteristics of the solutions were specified by a turbidimeter and a pH meter, respectively, maintaining turbidity and pH values. A VELP TB1 model turbidimeter was used to measure the turbidity value of the solutions with a measurement range of 0-1000 ntu (nephelometric turbidity unit). Acidic and basis characteristics of the final solution was determined by measuring its pH value with a WTW Inolab pH 720 model pH meter after the dispersion process.

A Perkin Elmer STA 6000 model DTA-TG instrument was used to identify thermal behavior of the dried powders from ambient temperature to 900 °C in air atmosphere with a heating rate of 10 °C/min. Solution evaporation, decomposition and phase formation of the powders were stated as a result of DTA-TG analysis. Prior to XRD analysis, the dried powders were calcined at 800 °C for 2 h resulting as final $Ca_{2.8}Pr_{0.2}Co_4O_9$ powders. XRD pattern of the final powders was identified by a Thermo Scientific ARL model X-ray diffractometer using Cu K_α irradiation (wavelength, $\lambda = 1.540562$ Å) in the range of $5° \leq 2\theta \leq 90°$ at a speed of 2°/min to state structural analysis. Elemental composition and element ratios of the powders were described using a A Thermo Scientific K-Alpha model XPS device with an Al K_α X-ray source between 0-1350 eV energy range.

As-obtained $Ca_{2.8}Pr_{0.2}Co_4O_9$ powders were pre-shaped by a mechanical press at 120 MPa. Next, the samples were subjected to HIP at 700 °C under Ar gas pressure of 100 MPa for 30 min to consolidate the samples using an AIP HP630 model HIP equipment. After consolidation, the bulk samples were treated for 20 h at 1173 K.

Seebeck coefficient of $Ca_{2.8}Pr_{0.2}Co_4O_9$ bulk samples were performed between 323 and 673 K using slope method at steady state conditions with a uniaxial 4-point contact arrangement. In this method, thermocouples are inserted through the heaters in direct contact with the sample [16]. In this study, Seebeck coefficient values of the samples were determined using chromel–Nb thermocouples by applying a temperature gradient between +7.5 K and -7.5 K throughout the samples.

3. RESULTS AND DISCUSSION

It is important to specify if powder precursors are dissolved completely in solutions in terms of obtaining homogeneous solutions. Within this context, turbidity measurements are performed by inspecting ntu values of the solutions in the range of 0-1000 ntu. A homogeneous solution has been formed if the turbidity value is reputed to be closer to 0, and powder precursors have not been dissolved entirely in solutions if the turbidity value is measured closer to 1000 [17]. In addition, gel formation is affected by the pH value of the solutions and the pH value ought to be regarded during solution preparation. In this work, turbidity and pH values of the prepared solution were found as 0.36 ntu and 1.19, respectively, meaning that the precursors were dissolved very well in the solution and the solution showed acidic characteristics forming a branched structure during the gelation process.

DTA-TG analysis was applied to the $Ca_{2.8}Pr_{0.2}Co_4O_9$ powders dried at 200 °C for 2 h in air with a heating rate of 10 °C per minute in air atmosphere until 900 °C and the results are shown in **Fig. 1**. Endothermic and exothermic reactions occur at the temperature range of 270 °C and 480 °C with reference to DTA curve in the figure. Exothermic peak between 270 °C and 300 is related to burning out of organic residuals containing C based materials. At the same temperature interval, a weight loss of 10% is stated from TG curve due to removal of organic groups. Endothermic peak between temperatures of 440 °C and 480 °C is regarded to oxidation of Ca, Pr, and Co. A significant weight loss of approximately 30% on the TG curve is observed due to these peaks. Phase formation of $Ca_{2.8}Pr_{0.2}Co_4O_9$ starts after 480 °C according to the DTA curve and small weight losses were observed depending on the phase formation.

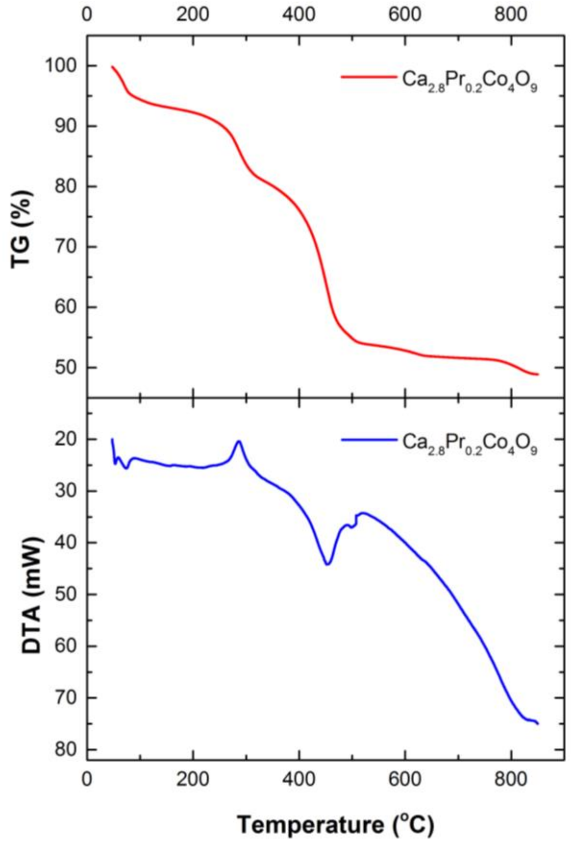

Figure 1. DTA and TG curves of $Ca_{2.8}Pr_{0.2}Co_4O_9$ powders dried at 200 °C in air.

XRD pattern of $Ca_{2.8}Pr_{0.2}Co_4O_9$ powders manufactured by sol-gel method is shown in **Fig. 2**. Formation of crystalline structure for $Ca_{2.8}Pr_{0.2}Co_4O_9$ particles was depicted with sharp diffraction peaks. 2θ peaks at 16.54°, 24.86°, 30.30°, 33.38°, 37.22°, 39.56°,43.46°, 48.68°, and 55.46° seen from the phase spectrum correspond to typical $Ca_3Co_4O_9$ peaks and are agreeable with the literature [18]. Any other phases were not observed in the XRD detection. In addition, average crystalline size of $Ca_{2.8}Pr_{0.2}Co_4O_9$ particles were determined using the intensities of the primary peaks of reflection at 2θ=33.38° by the Debye-Scherer equation [19] which is given as $D = 0.9\lambda/\beta cos\theta$. Here, D is the average crystalline size, λ is the X-ray wavelength, β is the full width at half the maximum intensity, and θ is the Bragg's diffraction angle. Average crystalline size of the $Ca_{2.8}Pr_{0.2}Co_4O_9$ particles was calculated as 27.6 nm using Debye-Scherer equation.

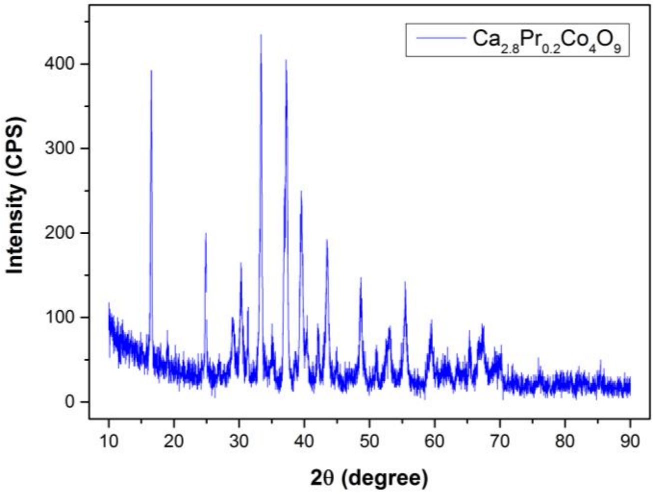

Figure 2. XRD spectra of $Ca_{2.8}Pr_{0.2}Co_4O_9$ powders calcined at 800 °C for 2 h in air.

A wide scan XPS spectra of $Ca_{2.8}Pr_{0.2}Co_4O_9$ powders was evaluated within the range of 0-1350 eV with an energy step size of 1.0 eV. According to in **Fig. 3**. Sharp peaks seen in the XPS spectra confirm that elements of Ca, Pr, Co, and O exist within the powder sample corresponding with the peaks. In addition, peaks corresponding to C and Cl are also detected in the spectra. Existence of Cl is the result of distilled water used to dissolve the precursors and C is the result of reaction with CO_2 in air. **Table 3** gives elemental analysis and quantification of $Ca_{2.8}Pr_{0.2}Co_4O_9$ powders including binding energies (BE) in eV with their corresponding full-width at half maximum (FWHM). Elemental analysis from XPS shows that $Ca_{2.8}Pr_{0.2}Co_4O_9$ powders consist of 14.25% Ca, 38.24% O, 7.21% Co, and 0.46% Pr. It can be noticed from the table that components of Ca 2p, O 1s, Co 2p, and Pr 4d are formed with binding energies of 346.21 eV, 530.05 eV, 780.23 eV, and 115.81 eV, respectively. Although effect of Pr doping cannot be detected in the XRD pattern, presence of Pr dopant can be detected in the XPS spectra. Hence, doping of Pr into $Ca_3Co_4O_9$ was successfully accomplished.

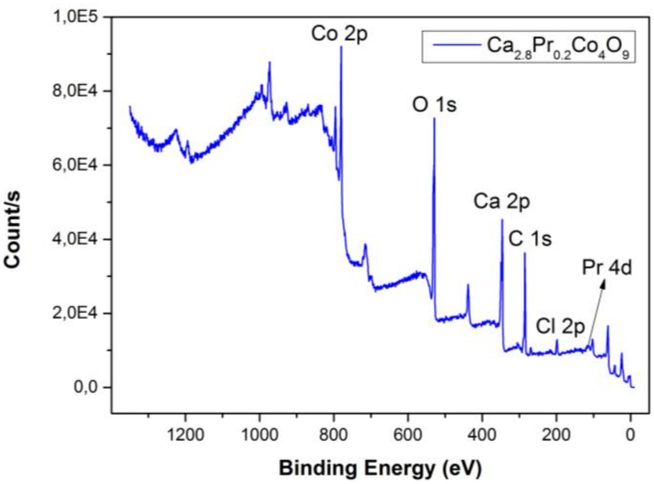

Figure 3. Wide survey XPS spectra of $Ca_{2.8}Pr_{0.2}Co_4O_9$ powders.

Table 3. Elemental analysis and quantification of $Ca_{2.8}Pr_{0.2}Co_4O_9$ powders.

Peak	**Position BE (eV)**	**FWHM (eV)**	**Area (cps eV)**	**Amount (%)**
Ca 2p	346.21	3.368	143301.59	14.25
O 1s	530.05	4.451	199972.85	38.24
Co 2p	780.23	3.072	205702.10	7.21
Pr 4d	115.81	3.811	7567.86	0.46

Seebeck coefficients of $Ca_{2.8}Pr_{0.2}Co_4O_9$ bulk samples are given in **Fig. 4** between 100 °C and 400 °C. Since the Seebeck coefficient of the samples are positive, the materials are p-type and holes are the dominant charge carriers. Behavior of Seebeck coefficient for $Ca_3Co_4O_9$ can be explained by Co^{+4} concentration based on CoO_2 layers [20]. Doping of Pr^{+3} instead of Ca^{+2} is considered to increase the hole concentration in the samples and thereby Co^{+4} concentration is decreased causing an increase in Seebeck coefficient. Compared to the literature values [20], Seebeck coefficients of the samples are much higher than $Ca_3Co_4O_9$ while they are closer to literature value of $Ca_{2.8}Pr_{0.2}Co_4O_9$. The highest Seebeck coefficient of $Ca_{2.8}Pr_{0.2}Co_4O_9$ is 179 μV/K at 400 °C which is a little higher than the literature value. These results show that Pr is an effective dopant to increase the Seebeck coefficient values. Overall, $Ca_{2.8}Pr_{0.2}Co_4O_9$ can be a promising p-type thermoelectric material.

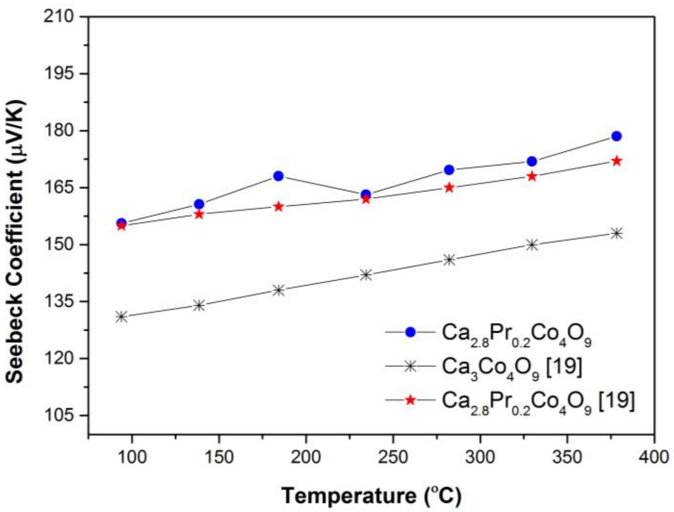

Figure 4. Temperature dependence of Seebeck coefficient for $Ca_{2.8}Pr_{0.2}Co_4O_9$.

4. CONCLUSIONS

This study contains successfully synthesis and characterization of $Ca_{2.8}Pr_{0.2}Co_4O_9$ powders for high temperature thermoelectric applications using sol-gel method following hot isostatic pressing. Drying, oxidation and phase transformation temperatures of the powders were optimized according to the DTA-TG and FTIR results. Formation of crystalline structure for $Ca_{2.8}Pr_{0.2}Co_4O_9$ particles was depicted with sharp diffraction peaks in the XRD pattern corresponding to typical $Ca_3Co_4O_9$ peaks compatible with the literature. In addition, average crystalline size of the $Ca_{2.8}Pr_{0.2}Co_4O_9$ particles was calculated as 27.6 nm using Debye-Scherer equation. Sharp peaks seen in the wide survey XPS spectra confirm that elements of Ca, Pr, Co, and O exist within the powder sample. Although effect of Pr doping cannot be detected in the XRD pattern, presence of Pr dopant can be detected in the XPS spectra. Hence, doping of Pr into $Ca_3Co_4O_9$ was successfully accomplished. Doping of Pr^{+3} instead of Ca^{+2} is considered to increase the hole concentration in the samples and resulted in an increase in Co^{+4} concentration. As a result, Seebeck coefficient of the samples increased with respect to the increase in Co^{+4} concentration. Seebeck coefficients of the samples are much higher than $Ca_3Co_4O_9$ while they are closer to literature value of $Ca_{2.8}Pr_{0.2}Co_4O_9$. Maximum Seebeck coefficient of the samples is found to be 179 μV/K at 400 °C. These results show that Pr is an effective dopant to increase the Seebeck coefficient values.

ACKNOWLEDGEMENTS

This work was supported by the Scientific and Technological Research Council of Turkey (TUBITAK) in Turkey under Project No. 115M579. We would like to thank the Center for Production and Application of Electronic Materials (EMUM) in Dokuz Eylul University in Izmir, Turkey for research collaboration. We appreciate Prof. G. J. Snyder and Dr. Umut Aydemir at Northwestern University in Evanston, IL, USA for Seebeck coefficient measurements.

REFERENCES

[1] J. Garcia-Canadas and G. Min, "Multifunctional probes for high-throughput measurement of Seebeck coefficient and electrical conductivity at room temperature," *Rev Sci Instrum,* vol. 85, p. 043906, Apr 2014.

[2] M. S. Dresselhaus, G. Chen, Z. F. Ren, G. Dresselhaus, A. Henry, and J.-P. Fleurial, "New Composite Thermoelectric Materials for Energy Harvesting Applications," *JOM,* vol. 61, pp. 86-90, 2009.

[3] S. Bhattacharya, S. Rayaprol, A. Singh, A. Dogra, C. Thinaharan, D. K. Aswal*, et al.*, "Low temperature thermopower and electrical transport in misfit Ca3Co4O9 with elongated c-axis," *Journal of Physics D: Applied Physics,* vol. 41, p. 085414, 2008.

[4] R. Funahashi, M. Mikami, T. Mihara, S. Urata, and N. Ando, "A portable thermoelectric-power-generating module composed of oxide devices," *Journal of Applied Physics,* vol. 99, p. 066117, 2006.

[5] Y. Song, Q. Sun, L. Zhao, F. Wang, and Z. Jiang, "Synthesis and thermoelectric power factor of (Ca0.95Bi0.05)3Co4O9/Ag composites," *Materials Chemistry and Physics,* vol. 113, pp. 645-649, 2009.

[6] L. Han, N. V. Nong, L. T. Hung, T. Holgate, N. Pryds, M. Ohtaki*, et al.*, "The influence of α- and γ-Al2O3 phases on the thermoelectric properties of Al-doped ZnO," *Journal of Alloys and Compounds,* vol. 555, pp. 291-296, 2013.

[7] H. Alam and S. Ramakrishna, "A review on the enhancement of figure of merit from bulk to nano-thermoelectric materials," *Nano Energy,* vol. 2, pp. 190-212, 2013.

[8] Y. Wang, Y. Sui, J. Cheng, X. Wang, and W. Su, "Comparison of the high temperature thermoelectric properties for Ag-doped and Ag-added Ca3Co4O9," *Journal of Alloys and Compounds,* vol. 477, pp. 817-821, 2009.

[9] N. Van Nong, N. Pryds, S. Linderoth, and M. Ohtaki, "Enhancement of the thermoelectric performance of p-type layered oxide Ca(3)Co(4)O((9)+delta) through heavy doping and metallic nanoinclusions," *Adv Mater,* vol. 23, pp. 2484-90, Jun 3 2011.

[10] C. Chen, T. Zhang, R. Donelson, D. Chu, R. Tian, T. T. Tan*, et al.*, "Thermopower and chemical stability of Na0.77CoO2/Ca3Co4O9 composites," *Acta Materialia,* vol. 63, pp. 99-106, 2014.

[11] H. Su, Y. Jiang, X. Lan, X. Liu, H. Zhong, and D. Yu, "Ca3 − xBixCo4O9 and Ca1 − ySmyMnO3 thermoelectric materials and their power-generation devices," *physica status solidi (a),* vol. 208, pp. 147-155, 2011.

[12] K. Park, H. K. Hwang, J. W. Seo, and W. S. Seo, "Enhanced high-temperature thermoelectric properties of Ce- and Dy-doped ZnO for power generation," *Energy,* vol. 54, pp. 139-145, 2013.

[13] S. W. Nan, J.; Deng, Y.; Nan, C.W., "Synthesis and thermoelectric properties of $(Na_xCa_{(1-x)})_3Co_4O_9$ ceramics," *Journal of the European Ceramic Society* vol. 23, pp. 859-863, 2003.

[14] A. Goktas, I. H. Mutlu, Y. Yamada, and E. Celik, "Influence of pH on the structural optical and magnetic properties of Zn1−xMnxO thin films grown by sol–gel method," *Journal of Alloys and Compounds,* vol. 553, pp. 259-266, 2013.

[15] M. H. Bocanegra-Bernal, "Hot Isostatic Pressing (HIP) technology and its applications to metals and ceramics," *Journal of Materials Science*, vol. 39, pp. 6399-6420, 2004.

[16] K. A. Borup, J. de Boor, H. Wang, F. Drymiotis, F. Gascoin, X. Shi, *et al.*, "Measuring thermoelectric transport properties of materials," *Energy Environ. Sci.*, vol. 8, pp. 423-435, 2015.

[17] E. Celik, U. Aybarc, M. F. Ebeoglugil, I. Birlik, and O. Culha, "ITO films on glass substrate by sol–gel technique: synthesis, characterization and optical properties," *Journal of Sol-Gel Science and Technology*, vol. 50, pp. 337-347, 2009.

[18] H. Q. Liu, X. B. Zhao, T. J. Zhu, Y. Song, and F. P. Wang, "Thermoelectric properties of Gd, Y co-doped Ca3Co4O9+δ," *Current Applied Physics*, vol. 9, pp. 409-413, 2009.

[19] M. Rezaei, M. Khajenoori, and B. Nematollahi, "Preparation of nanocrystalline MgO by surfactant assisted precipitation method," *Materials Research Bulletin*, vol. 46, pp. 1632-1637, 2011.

[20] F. P. Zhang, X. Zhang, Q. M. Lu, J. X. Zhang, Y. Q. Liu, and G. Z. Zhang, "Effects of Pr doping on thermoelectric transport properties of Ca3−xPrxCo4O9," *Solid State Sciences*, vol. 13, pp. 1443-1447, 2011.